Joint Bistatic Low Frequency Airborne Radar Experiments

LARS M.H. ULANDER, BJÖRN FLOOD, PER-OLOV FRÖLIND,
ANDERS GUSTAVSSON, TOMMY JONSSON, BJÖRN LARSSON,
MIKAEL LUNDBERG, DANIEL MURDIN, ROLF RAGNARSSON,
GUNNAR STENSTRÖM, PHILIPPE DREUILLET, PHILIPPE MARTINEAU,
OLIVIER RUAULT DU PLESSIS, AND BERNARD VAIZAN

FOI, Swedish Defence Research Agency, is a mainly assignment-funded agency under the Ministry of Defence. The core activities are research, method and technology development, as well as studies conducted in the interests of Swedish defence and the safety and security of society. The organisation employs approximately 1000 personnel of whom about 800 are scientists. This makes FOI Sweden's largest research institute. FOI gives its customers access to leading-edge expertise in a large number of fields such as security policy studies, defence and security related analyses, the assessment of various types of threat, systems for control and management of crises, protection against and management of hazardous substances, IT security and the potential offered by new sensors.

FOI
Defence Research Agency
Information Systems
Box 1165
SE-581 11 Linköping

Phone: +46 13 37 80 00
Fax: +46 13 37 81 00

www.foi.se

FOI-R--3274--SE
ISSN 1650-1942

Technical report
September 2011

Information Systems

Lars M.H. Ulander, Björn Flood, Per-Olov Frölind,
Anders Gustavsson, Tommy Jonsson,
Björn Larsson, Mikael Lundberg, Daniel Murdin,
Rolf Ragnarsson, Gunnar Stenström, Philippe
Dreuillet, Philippe Martineau, Olivier Ruault du
Plessis, and Bernard Vaizan

Joint Bistatic Low Frequency Airborne Radar Experiments

Titel	Gemensamt test av bistatisk lågfrekvent flygburen radar
Title	Joint bistatic low frequency airborne radar experiments
Rapportnr/Report no	FOI-R--3274--SE
Rapporttyp/ Report Type	Teknisk Rapport/ Technical Report
Sidor/Pages	25 p
Månad/Month	September/ September
Utgivningsår/Year	2011
ISSN	ISSN 1650-1942
Kund/Customer	Försvarsmakten/ Swedish Armed Forces
Projektnr/Project no	E53052
Godkänd av/Approved by	Lars Bohman

FOI, Totalförsvarets Forskningsinstitut
Avdelningen för Informationssystem
Box 1165
581 11 Linköping

FOI, Swedish Defence Research Agency
Information Systems
Box 1165
SE-581 11 Linköping

Sammanfattning

Rapporten beskriver det fransk-svenska bilaterala forskningsprojektet “Gemensamt test av bistatisk lågfrekvent flygburen radar” och sammanfattar de viktigaste resultaten. Projektet har utvecklat, testat och demonstrerat bistatisk syntetisk apertur radar (SAR) för VHF/UHF-bandet (222-460 MHz) med sändare och mottagare på två flygplan. Konceptet testades första gången i Frankrike 2009 and sedan genomfördes en omfattande datainsamling i Sverige 2010.

Datainsamlingen 2010 demonstrerade för första gången att bistatiska SAR-bilder kan produceras med liknande kvalité som monostatiska SAR-bilder på VHF/UHF-bandet. Teknikerna som utvecklats för att synkronisera systemen fungerade tillfredsställande och den uppnådda bildupplösningen blev enligt förväntan. Den geometriska noggrannheten av de bistatiska bilderna var något sämre än i de monostatiska bilderna vilket försvårade förändringsdetektion. Orsaken till problemet är inte helt klarlagt men beror förmodligen på kvarvarande fasdrift mellan systemen.

De flesta flygningarna genomfördes med de två flygplanen sida-vid-sida och med samma fart utefter parallellförflyttade banor. Den bistatiska elevationsvinkeln varierades mellan 0° (“kvasi-monostatisk”) och 10°. Ytterligare några geometrier studerades såsom cirkelbanor, kombination av cirkulär och rak bana, samt parallella banor med olika fart.

Det primära försöksområdet var markstridskolan i Kvarn där mål arrangerades på öppna fält och dolda i skogen. Försöket inkluderade också ett område med byggnader som var under uppförande. Ett andra försöksområde var Remningstorp, strax väster om Skövde i Västra Götaland, som är en skoglig försökspark med en omfattande databas av skogliga parametrar.

Resultaten från både Kvarn och Remningstorp visar att klotternivån över skogen minskar i de bistatiska bilderna (horisontell polarisation). Undertryckningen av klotter är upp till 10 dB och ökar när den bistatiska elevationsvinkeln ökar. De dolda målen påverkas i mindre omfattning vilket innebär att mål-bakgrund-kontrasten i allmänhet ökar och därmed detektionsprestanda.

Resultat från bebyggelsen i Kvarn visar att penetration genom icke-metalliska tak och avbildning av interiörer är möjliga med SAR på VHF/UHF-bandet.

Nyckelord: Radar, bistatisk, SAR, VHF-band, UHF-band

Summary

The French-Swedish bilateral research project “Joint Bistatic Low Frequency Airborne Radar Experiments” is described and the main results summarised. The project has developed, tested and demonstrated bistatic synthetic aperture radar (SAR) operating in the VHF/UHF-band (222-460 MHz) with transmitter and receiver on two airborne platforms. The concept was first tested in France 2009 and then an extensive data collection was performed in Sweden 2010.

The data collection in 2010 demonstrated for the first time that bistatic SAR images can be generated with similar quality as monostatic SAR images in the VHF/UHF-band. The techniques developed to synchronise the radar systems worked successfully and images with nominal resolution were obtained. The geometrical accuracy of the bistatic images is slightly inferior compared to the monostatic images which reduces change detection performance. The cause of this problem is not fully understood but it is likely due to residual phase drift between the radar systems.

Most of the flights were conducted with the two aircraft flying side-by-side with the same velocity along parallel but offset tracks. Bistatic elevation angles between 0° (“quasi-monostatic”) and 10° were realised in this manner. A few other geometries were also used, i.e. circular tracks, combinations of circular and straight tracks as well as parallel tracks with different speeds.

The main test site of the experiment was the Swedish Army Combat School at Kvarn where targets were deployed in the open and concealed in forests. The site also included an area with buildings under construction. The second test site used was Remningstorp, west of the city of Skövde in Västra Götaland, which is a forest research park with an extensive data base of forest parameters.

Results from both Kvarn and Remningstorp show that the bistatic images (horizontal polarisation) show a decrease of the forest clutter. The effect is more pronounced when the bistatic elevation angle increases and a suppression of up to 10 dB is observed. The concealed targets are less affected which means that the target-to-clutter ratio generally increases and hence detection performance.

Results from the building complex in Kvarn show that penetration through non-metallic roofs of buildings and imaging of building interiors are possible using VHF/UHF-band SAR.

Keywords: Radar, bistatic, SAR, VHF-band, UHF-band

Innehållsförteckning

1 Introduction

The report summarizes the research collaboration “Joint Bistatic Low Frequency Airborne Radar Experiments” between DGA and ONERA in France and FOI in Sweden [1]. The objective has been to evaluate the performance of bistatic low-frequency airborne synthetic aperture radar (SAR) for foliage penetration and urban applications. The research has investigated detection of targets concealed in dense forests as well as penetration into buildings using two cooperating radars, i.e. the French SETHI and the Swedish LORA.

A bistatic radar is based on using transmit and receive antennas at separated locations as opposed to a monostatic radar where the two antennas are co-located or a single antenna is used for transmit and receive. Bistatic radar has been studied since the earliest days of radar development in the 1930’s. However, there are still few bistatic radars in comparison with the total number of operational radar systems, most likely due to technical challenges concerning synchronization. More details on both historical and contemporary bistatic radar developments can be found in [2][3]. Examples of bistatic SAR at X-band using two airborne platforms or a mix of spaceborne and airborne platforms are given in [4][5].

Bistatic radar offers several advantages compared to monostatic radar. For defence purposes, the most important one is the possibility to obtain radar data using a passive sensor. By separating the transmitting and receiving parts onto different platforms it is possible to move the former to a position at a longer distance (*sanctuary*) from a hostile threat. The platform with the receiving part is passive and does not radiate signals which can be intercepted. It can therefore be operated at a closer range to a hostile threat.

The term low-frequency radar is used in this report to describe systems with operating frequency below the traditional microwave band, i.e. below 1 GHz. It is known from past research that low-frequency SAR provides significant penetration into forests and enables detection of concealed vehicle-sized targets using change detection techniques [6][7]. A review of foliage penetration radar (FOPEN) is available in a recent book [8].

Several tests with monostatic low-frequency SAR have been performed in the past to quantify the performance of detecting concealed targets [6][7][9][10][11][12][13]. The conclusion is that the band 25-85 MHz gives the overall best detection performance for truck-sized targets but that detection performance decreases for larger incidence angles since the target radar-cross section (RCS) is reduced by ground-reflection interference. Detection results for the higher band 200-500 MHz are generally inferior due to higher clutter levels and target fading with aspect angle. The higher band, however, provides comparatively better performance for larger incidence angles and smaller targets.

In contrast to the FOPEN application, little is known about the capability of a low-frequency SAR to penetrate and image targets inside buildings. Only limited results are available in the open literature, e.g. attenuation through different materials or results obtained from SAR simulations [14][15][16][17]. The results given here based on real SAR data for this application will consequently be exploratory in nature.

Combining bistatic geometries with low-frequency SAR opens a possibility to increase target-to-clutter-ratio and improve detection. Monostatic HH-polarised clutter is often dominated by double-bounce reflection between horizontal ground and large vertical structures like tree stems or building walls. The mechanism decreases for bistatic geometries with elevation angle separation [18]. A target is less affected due to its lower height and target-to-clutter ratio as well as detection performance is expected to increase. A first verification of this idea was performed in 2007 using an airborne transmitter and a ground-based receiver in the band 28-73 MHz [19]. Results showed that target-to-clutter ratio increased up to 10 dB but image quality was far from optimum. The present research aims to demonstrate increased target-to-clutter ratio and evaluate the concept of operations in a bistatic geometry using two aircraft. The common frequency band was chosen to be within 200-500 MHz since LORA already operated in this band and SETHI was planned to be upgraded. Results from the first flight tests in 2009 have been reported in [20].

2 Airborne bistatic SAR

The concept of operating a bistatic SAR is illustrated in Figure 1, i.e. two cooperating radar systems which are located on separate airborne platforms. The illustration shows the transmitting part on-board an aircraft at large distance and the receiving part on-board a small UAV at close range. This configuration improves system survival by moving the vulnerable transmitter away from the imaged area.

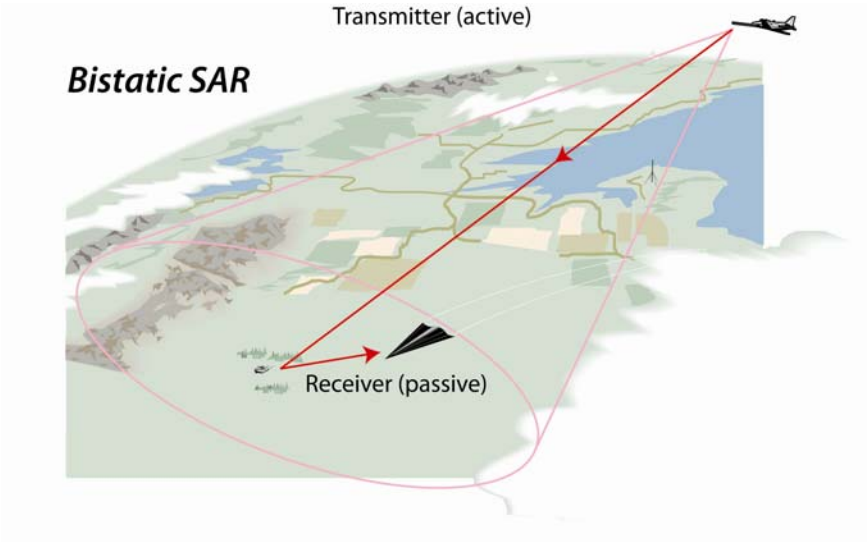

Figure 1. Example of bistatic SAR operation. The transmitter is located on a large platform at a long distance from the imaged area, whereas the receiver is located on a small platform at close range.

To the author's knowledge, it is the first time that a bistatic SAR system at low frequencies has been developed and operated. It is based on the French radar SETHI integrated on a Falcon 20 and the Swedish radar LORA integrated on a Saberliner, see Figure 2. They operate as a coherent bistatic system and cover 220-460 MHz. The lower limit is defined by the lowest useable frequency of the LORA antenna whereas the upper limit was selected to avoid transmitting into the digital TV broadcasting band starting at 470 MHz.

ONERA (French Aerospace Laboratory) has developed the SETHI airborne SAR system [21]. It uses two wing pods which are able to carry different payloads, i.e. radar antennas operating from the VHF- to X-band and/or optical sensors, and provides a wide range of acquisition geometries. The pod-based concept allows easy integration and testing using a single airworthiness certification. The antenna of the VHF/UHF-band radar developed for the bistatic experiments consists of a fully polarimetric antenna which is integrated into the left pod.

FOI (Swedish Defence Research Agency) has developed the LORA radar system [22]. LORA is designed to cover the band 200-800 MHz. The antenna system is integrated into two push booms located in front of the Saberliner nose. Each boom houses a left-looking five-element array covering 220-435 MHz and 435-800 MHz in the left and right booms, respectively. Only two elements - one for transmission and one for reception - are active in each boom during SAR operation. The antenna elements are bicones oriented along the axis of the booms and with a directive reflector behind. The polarization of this configuration is mainly horizontal but some vertical component is also generated which increases for larger Doppler frequency and depression angle.

In principle, the combined antenna polarization used for bistatic operation can be either horizontal-horizontal or vertical-horizontal since SETHI has a fully polarimetric antenna whereas LORA's antenna provides essentially horizontal polarization. The polarization

was chosen to be horizontal-horizontal during LORAMbis 2010 since simulations and experience showed that it would be more favourable. Vertical-horizontal was used in 2009 which indicated poor target-to-clutter contrasts [20].

(a) (b)

Figure 2. The two aircraft used in the bistatic experiments: (a) Falcon 20 with the SETHI radar where the antennas are mounted inside wing pods; (b) Sabreliner with the LORA radar and two push-boom antennas. (Photo to the right: Pia Ericson, FMV).

One of the main challenges for bistatic radar is to enable synchronization and maintain coherence between the two systems since they are not physically connected to each other. An important development during the project has therefore been to upgrade both systems with a GPS-disciplined oscillator. The latter uses the GPS 1-PPS (pulse-per-second) signal to control the master oscillator frequency of each system. This removes most of the oscillator drift between the two systems but a final correction is needed during signal processing. This correction can be estimated by recording the received direct signal of the transmitted pulse. Another important upgrade has been to enable fully coherent operation of LORA based on an oscillator bank instead of a frequency synthesizer as used in the past. The synchronization between the two systems is further complicated by the fact that LORA uses a stepped-frequency waveform to cover the full bandwidth. The developed solution is to define the waveform sequence with the same starting frequency for each 1-PPS pulse.

The formation of bistatic SAR images presents an additional challenge compared to monostatic data. The signal processing has therefore been upgraded to take into account two antenna positions and two master oscillators instead of a single one as in a monostatic system.

3 Development and initial testing

Measurements with the two radar systems SETHI and LORA were performed at two occasions in preparation for the main bistatic flight campaign in 2010.

In November 2008 tests of the proposed solution for time and frequency synchronization were performed in the laboratory at ONERA in Salon de Provence, France. The requirements of synchronicity between the two radar systems are imposed by several factors:

- **Stepped-frequency waveform**. The receiving radar unit has to be tuned to the same sub-band that was used for the latest radar pulse emitted by the transmitter.
- **Time synchronization**. During an imaging pass the drift between the trigger that positions the sampling window in the receiving system and the pulse repetition frequency (PRF) of the transmitter must be sufficiently low.
- **Phase synchronization**. The SETHI and LORA signals have to be in phase during each imaging pass to preserve a coherent registration and enable focusing in the bistatic SAR image formation.

For the laboratory tests SETHI and LORA had been equipped with an electronic board where a master oscillator of 10 MHz is controlled through a feedback loop by a 1-PPS signal retrieved and provided through a high quality GPS receiver available in both systems. This hardware implementation had been used earlier by FOI with good results during the bistatic SAR measurements at VHF-band [19]. The tests showed that a sufficient stability could be achieved but required a warming-up period of the board, preferably in the order of 15 to 30 minutes. The maximum drift between the 1-PPS system triggers was found to be 150 ns during 3 hours of measurements, see Figure 3. With a pulse length of 5 μs and a sampling window of 35 μs planned for the airborne measurements this value was acceptable. The defined stepped-frequency waveform was also verified to work properly during the tests with both SETHI and LORA acting transmitter or receiver. The waveform consists of four overlapping sub-bands that cover 222-460 MHz. A more detailed description of the laboratory tests is available in [23].

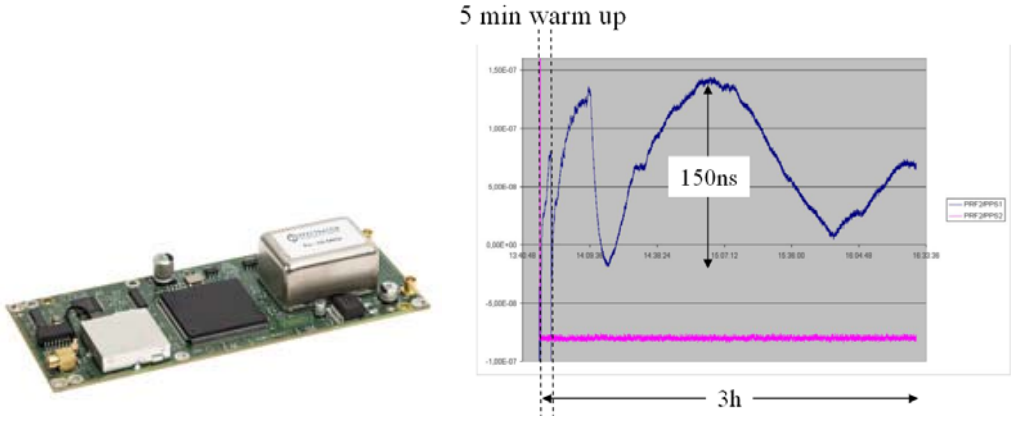

Figure 3. The commercially available board (EB03) integrated in both SETHI and LORA that contains the 10 MHz reference oscillator disciplined by the 1-PPS signal (left). Three hours of measurements of the drift between the two 1-PPS signals provided by the GPS receiver in each radar system (right).

The first airborne proof-of-concept and verification tests (LORAMbis 2009) were undertaken during one week in December 2009 [20]. The primary campaign objectives were to evaluate the implemented synchronization principle based on the experiences gained from the laboratory tests the year before and to examine the image quality obtained with the acquired bistatic VHF/UHF SAR data.

A test site close to Mende in southern France was selected. It is located about 1000 m above sea level and was used during an earlier common SAR experiment in 1998 [24]. Mende is quite close to Nîmes-Garons airport where the LORA and SETHI aircraft were based during the campaign. One of the reasons for selecting this area was to minimise radio-frequency interference (RFI). Another reason was the availability of ground truth information.

System checks were made on ground before the first flight. The transmitted waveform generated by SETHI was injected using a cable into the receiving system of LORA where it was digitized and stored on disk as a reference and calibration signal to be used in the bistatic SAR processing, see Figure 4. The same procedure was repeated but shifting the transmitting and receiving radar system. The flight program consisted of two identical missions with eight imaging passes in each. The bistatic geometry was limited to parallel tracks with a realization of four different bistatic elevation angles, i.e. 0° (“quasi-monostatic”), 3°, 6° and 10°. The imaging was repeated twice with SETHI as transmitter and LORA passive receiver during one pass and vice versa in the other.

The raw data set acquired over Mende could successfully be processed into bistatic SAR images and proved that the synchronization solution was good enough to work properly. Figure 4 shows a geo-referenced bistatic SAR image example registered over Mende and presented as an overlay on a map of the area.

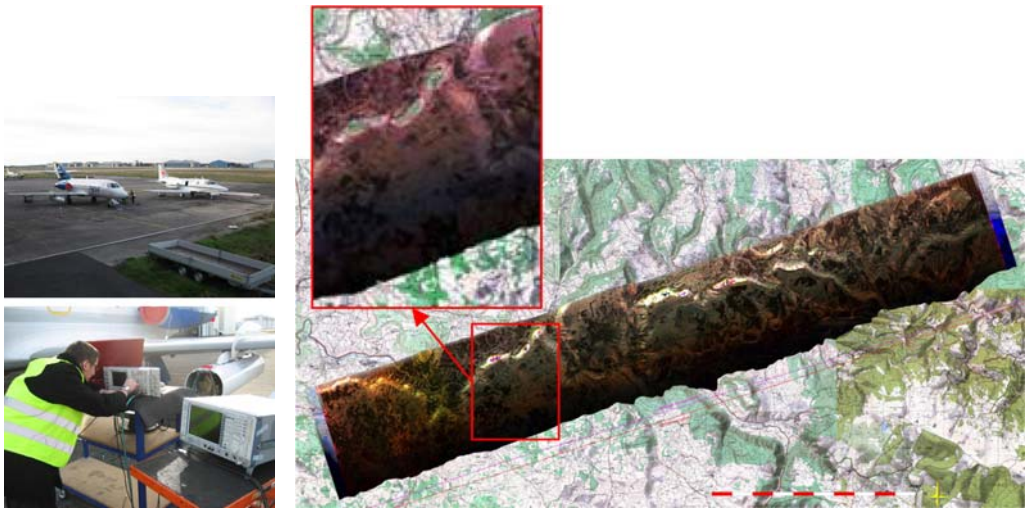

Figure 4. System calibration measurements with SETHI and LORA at Nîmes-Garons airport in preparation of the first flight mission during the campaign LORAMbis 2009 (left). Bistatic data acquired by SETHI with a bistatic elevation angle of 0° (“quasi-monostatic”) and formed into a SAR image which is visualized on top of a map covering the area (right). The significant topographic relief of the test size is clearly visible. Three of the four different sub-bands in the stepped-frequency waveform have in this case been processed separately instead of the fully reconstructed signal bandwidth. The colour coding based on the three sub-bands is 222-305 MHz (red), 272-355 MHz (green) and 400-460 MHz (blue).

4 Data collection LORAMbis 2010

The bistatic SAR experiment LORAMbis 2010 took place in southern Sweden during approximately two weeks, i.e. 20-30 September 2010. The main experiment objective was to study bistatic VHF/UHF SAR from an operational point of view with the application of target detection in forest concealment or urban environments in focus. Two different test sites were mapped by SETHI and LORA, i.e. Kvarn and Remningstorp.

4.1 Kvarn test site

Kvarn is part of the training range Prästtomta and located about 30 km northwest of the military airfield Malmen where the two aircraft were based during the bistatic SAR campaign in Sweden. Prästtomta is about 7400 ha large with open fields, meadows, marshes, forests and several small lakes. The forest stands exhibit a wide range of ages and are dominated by coniferous species. The ground elevation varies from 50 m to 120 m above sea level. Deployments of vehicle-sized targets under foliage were carried out at this test site. The forest area used for this was the same as one of three used during the French-Swedish SAR campaign LORAM conducted in 2004 [25]. It is marked in the aerial photo of Figure 5. During the first week of LORAMbis 2010 two bistatic flight missions were made with deployment A in place on ground and during the second week the same flight program was repeated but now with deployment B. The schematic map in Figure 5 shows the approximate locations for the sixteen terrain vehicles and one personal car used in the deployments with two symbol colours to distinguish A from B. The imaged area also covers a ground segment with a variety of building types which enables studies on bistatic clutter characteristics for this kind of environment.

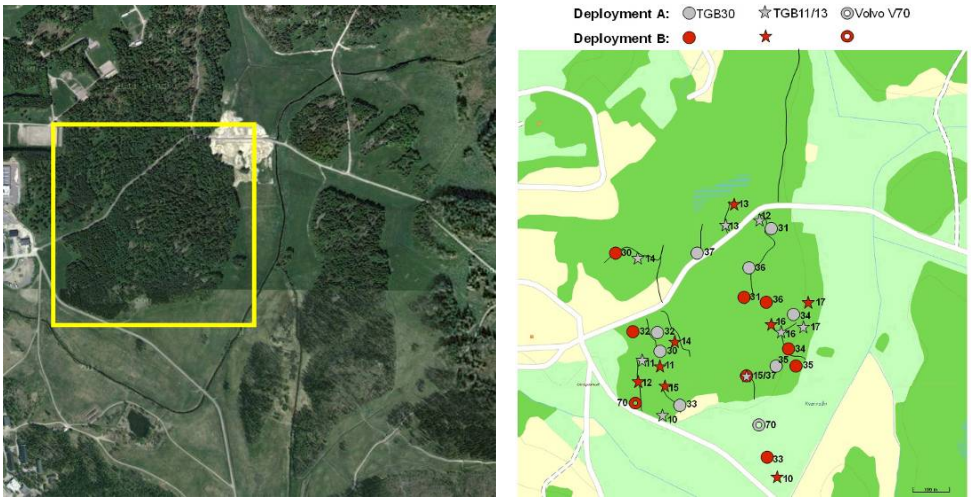

Figure 5. The coverage of the optical image (left) corresponds to the monostatic and bistatic SAR images in Figure 9 and is 2 km x 2 km large. The forest area used for the target deployment A and B during the campaign is marked by the yellow square. The schematic map (right) shows approximately the different locations used for the deployed targets with different symbols representing vehicle types and the gray and red symbol colour corresponds to deployment A and B, respectively. (Optical image: ©2011 Google - Imagery ©2011 DigitalGlobe, Cnes/Spot Image, GeoEye, Lantmäteriet/Metria).

Two terrain vehicles of a model type known as TGB11 in the Swedish Army were used and can be recognized as a small target class. The TGB11 has jeep-like dimensions but squeezed into a more cubic shape, i.e. 4.4 m long, 1.9 m wide and 2.2 m high. The primary use of the TGB11 is transportation of military personnel. Another vehicle type in the small target class is TGB13. It has the same basic design as TGB11 but is extended in length about one meter and equipped with a third axle in the rear. Six units of this type were included. The third terrain vehicle model type used was TGB30 with a truck-like design.

This vehicle has a length of 6.8 m, a width of 2.5 m and a height of 2.9 m. It comprises a medium target class. Eight TGB30 were available during the campaign. Different versions of the TGB30 exist depending upon the configuration of its truck bed but was similar for all eight in this case. Finally, the personal car was a Volvo station wagon and thus a small target class. Figure 6 shows photos of all four types captured during deployment B. The majority of locations were the same as during the earlier campaign LORAM in 2004 with positions accurately measured by a land surveyor. The positions of the new locations introduced have been retrieved from LiDAR measurements conducted for both deployment A and B using a helicopterborne laser scanner.

Figure 6. The target types used in the LORAMbis 2010 deployments, i.e. TGB30 (top, left), TGB13 (top, right), TGB11 (bottom, left) and Volvo station wagon (bottom, right).

4.2 Remningstorp test site

The second test site Remningstorp covers about 1200 ha of productive forest land divided into over 300 stands. The dominating tree species are Norway spruce (*Picea abies* (L.) Karst.), Scots pine (*Pinus sylvestris* L.) and birch (*Betula* spp.). It is mainly a production forest with stem volume varying up to 600 m^3/ha on stand level. The variability of forest characteristics is well documented in terms of different forest parameters. The area is overall rather flat with a topographic elevation range of about 20 m. Remningstorp was mapped during one bistatic flight mission with the objective to collect a data set where forest clutter characteristics can be studied in detail with access to detailed ground truth.

4.3 Bistatic flight geometries

Four different types of flight geometries were used during LORAMbis 2010 and are shown in Figure 7. In most cases, the flight altitude for the transmitting aircraft was 10000 ft and 11000 ft for the receiving aircraft. The majority of the imaging passes were devoted to parallel and offset tracks within visual range and all of the results presented in this report are from this geometry, i.e. a bistatic elevation angle of 0° (“quasi-monostatic”), 3°, 6° or 10°. The defined elevation angles are valid at the radar aim point in the centre of the imaged ground scene and will vary across the swath width, see Figure 8.

In general, the geometries were flown with SETHI as transmitter and LORA as receiver, as well as vice versa. In Remningstorp with one flight mission only the imaging geometries were limited to the two found to the left in Figure 7. The number of imaging passes conducted in one flight mission was about ten. Only a few of all monostatic and bistatic data registrations planned could not be completed successfully.

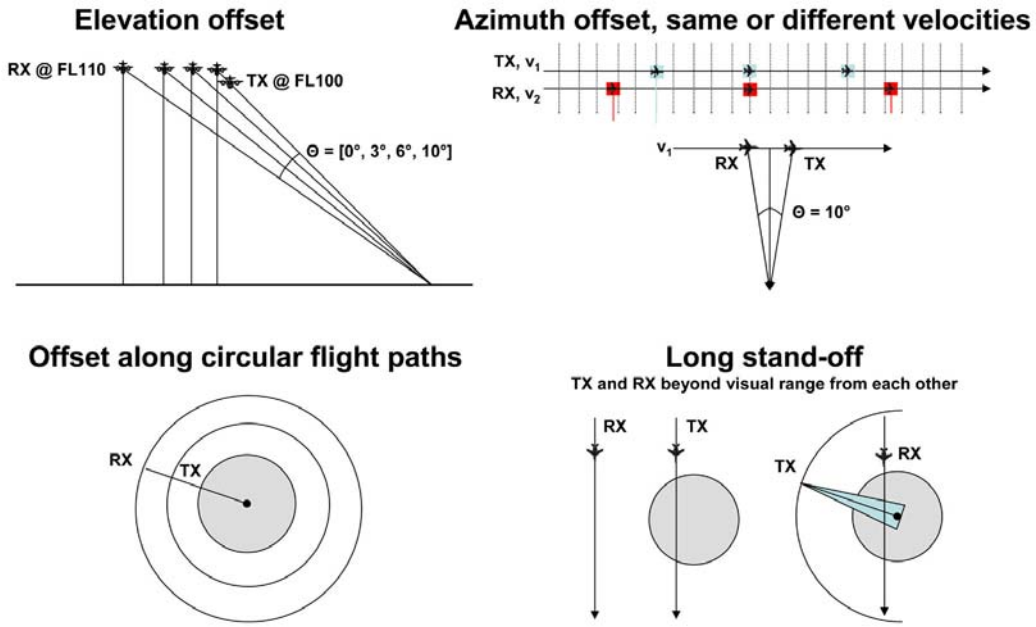

Figure 7. The four types of bistatic flight geometries used during LORAMbis 2010. For the imaging passes with variations the in bistatic elevation angle the same figures were used as in the first bistatic airborne tests conducted in France the year before, i.e. 0° (“quasi-monostatic”), 3°, 6° and 10°.

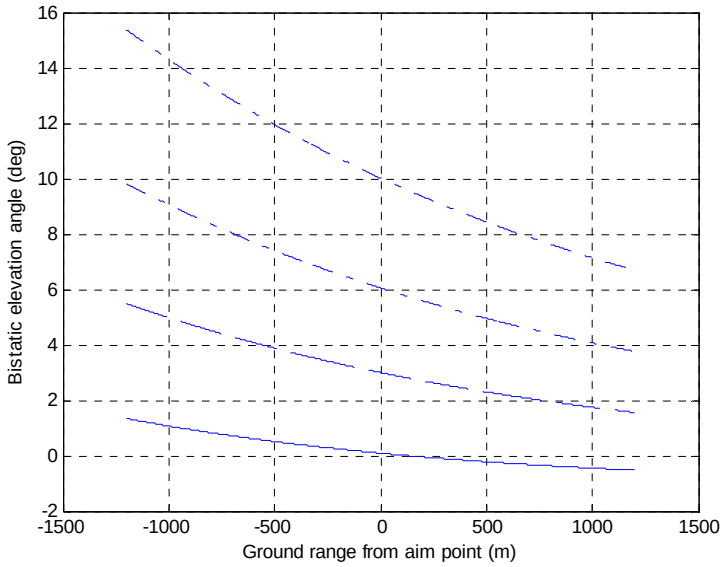

Figure 8. The bistatic elevation angle varies across the imaged swath. It is equal to the nominal value only when the ground range is the same as the ground range at the aim point. The four curves correspond to the angles defined for the LORAMbis 2010 bistatic SAR acquisition geometries, i.e. 0° (“quasi-monostatic”), 3°, 6° and 10° at the aim point.

5 Results

In this section we include both mono- and bistatic results from the LORAMbis 2010 data collection in the form of image examples and some quality measures. The latter is, however, only given for data recorded by the LORA system in this report.

5.1 FOI LORA image examples

Processing of bistatic SAR data is much more challenging than monostatic data but we will, based on data registered by LORA, demonstrate that the resulting quality of the bistatic images is in parity to the monostatic images. Besides the theoretical challenge of inverting bistatic data and formulating an efficient image formation algorithm, bistatic SAR processing needs information on antenna position of both systems and to properly deal with time synchronization and correct for oscillator drift between the systems. The latter can be done in different ways but the preferred method is to transfer the transmit phase information to the receiving system. A data link was not available in the LORAMbis 2010 data collection but the LORA system received and recorded the transmitted (direct) signal by SETHI which enabled the relative transmit phase to be retrieved. The quality of retrieval varied since the amplitude of the direct signal varied due to antenna gain variations during a data collection. The image formation is performed using the fast factorized backprojection algorithm developed for monostatic SAR but generalized to the bistatic case [26][27].

The first example in Figure 9 shows a comparison between a monostatic and two bistatic SAR images which cover the same area as shown in Figure 5. The left (monostatic) and middle (bistatic elevation angle 0°) images are similar and both show strong clutter over most of the forested areas as well as the buildings due to double-bounce scattering between the ground and the vertical structures. The clutter is particularly strong in areas where the ground is flat and horizontal. The bistatic image on the right, on the other hand, has a bistatic elevation angle of 10° and the corresponding clutter statistics has changed with the largest reduction in the areas with strong clutter. The observation is explained by the bistatic geometry which reduces the double-bounce scattering [28]. Only a small fraction of the forested areas have unchanged or slightly stronger clutter, most likely due to weak double-bounce in the monostatic image. Images corresponding to bistatic elevation angles of 3° and 6° (not shown) show clutter suppression in between the results for 0° and 10°. The results demonstrate that the clutter is reduced for these bistatic SAR geometries.

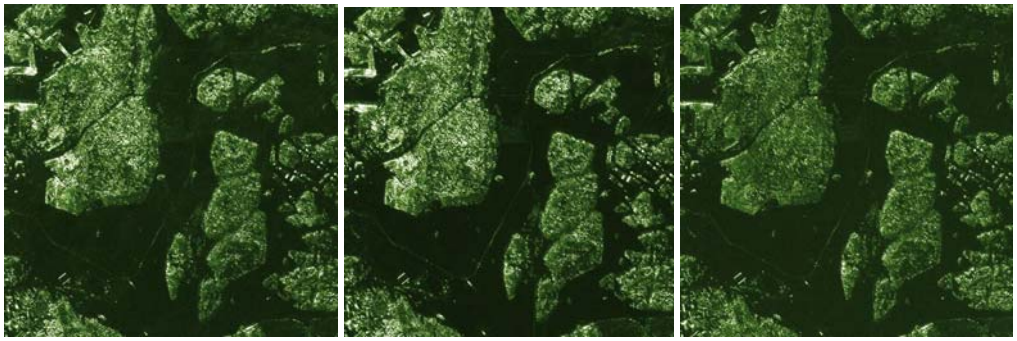

(a) Mission 1 Pass 2 (b) Mission 1 Pass 4 (c) Mission 2 Pass 6

Figure 9. (a) Monostatic LORA image. (b)-(c) Bistatic image with LORA as receiver and SETHI as transmitter. Bistatic elevation angle is 0° in (b) and 10° in (c). Kvarn test site, flight heading 225° and radar antenna is left looking. The image size is 2 km x 2 km.

The second example in Figure 10 is from the second test site Remningstorp: (a) is a monostatic image and (b) is a bistatic image with bistatic elevation angle of 6°. Again, significant clutter suppression is observed due to reduction of double-bounce scattering between the ground and the trees. The clutter suppression is even more pronounced compared to the examples from Kvarn in Figure 9. The reason is that Remningstorp has less topography than Kvarn. However, ground slopes can locally be steep which also is reflected in the images.

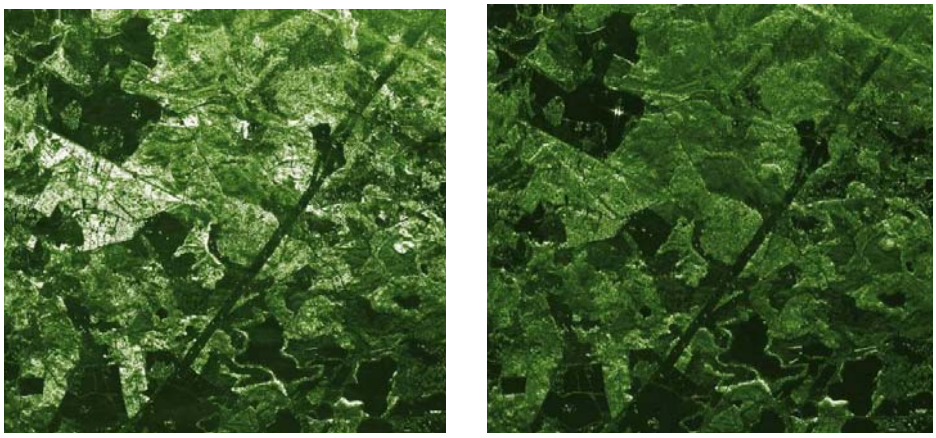

(a) Mission 5 Pass 2 (b) Mission 5 Pass 6

Figure 10. (a) Monostatic LORA image of Remningstorp. (b) Bistatic image with LORA as receiver and SETHI as transmitter. Bistatic elevation angle is 6° in (b). Flight heading 268° and radar is left looking. The image size is 3.6 km x 3.5 km.

5.2 ONERA SETHI image examples

Examples of mono- and bistatic images with SETHI as receiver and LORA as transmitter for the test site Kvarn are given in Figure 11. The left image (a) is a monostatic image, whereas (b) and (c) correspond to 6° and 10° bistatic elevation angle.

The images have been formed with a SAR processor based on the range migration algorithm (RMA) for monostatic images and with an existing bistatic processor, originally used for bistatic experiments at X band, but here adapted to UHF band [29].

Although not clearly visible in Figure 11 due to the gray-scale coding applied, clutter suppression is observed when comparing forest clutter statistics between the mono- and bistatic images. It can also noticed that the signature of the vehicles in the open area (red circles) are very similar when comparing the mono- and bistatic results. This is in agreement with the expected behaviour of bistatic signatures at UHF-band for objects having a fairly low extent in the vertical direction and found on a horizontal ground.

(a) Mission 3 Pass 4 Deployment 2	(b) Mission 3 Pass 8 Deployment 2	(c) Mission 4 Pass 8 Deployment 2

Figure 11. (a) Monostatic SETHI image of Kvarn. (b) and (c) are bistatic images (6° and 10°) with SETHI as receiver and LORA as transmitter. Flight heading 225° and radar is left looking. The image size is 1.4 km x 1.4 km.

5.3 Direct signal characteristics

The transmitted (direct) signal by SETHI was recorded in imaging passes where LORA was receiver. Together with platform position data, it is possible to track the phase drift between the systems and use it as a correction in the image formation process. Several tracking methods have been evaluated. All methods depend on good signal-to-noise ratio (SNR) and problems occur when the signal becomes weak due to signal fading. SNR variations are observed, see examples in Figure 12, and it is recommended for future experiments that measures are taken to minimise the signal fluctuations.

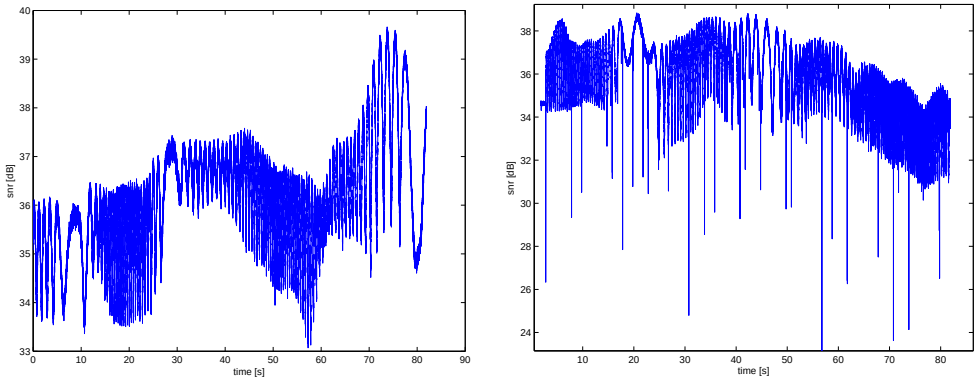

Figure 12. The plots show the signal-to-noise ratio (SNR) of the direct signal during two passes (bistatic elevation angle 0° and flight heading 315°). The left plot is from deployment A whereas the right plot is from deployment B. The plots show that SNR varies during a single pass due to fading through the antenna backlobe. The right plot also shows low values intermittently which may indicate system problems.

5.4 Image quality

The image examples in Section 5.1 indicate that the mono- and bistatic images have similar quality in terms of sensitivity and dynamic range. The image quality has also been assessed by measuring the response to trihedral radar reflectors. The side length of the reflectors is 5 m, i.e. much larger than the wavelength implying that they are essentially point targets close to the direction of maximum radar cross section. Representative examples of trihedral responses are shown in Figure 13. The main conclusion from the

analysis is that all monostatic images show similar image quality in terms of resolution and sidelobes. For the bistatic images, image quality shows more variability with the best image quality obtained for deployment A. It is presently not clear why the image quality for deployment B is worse but a possible explanation is uncompensated phase drift.

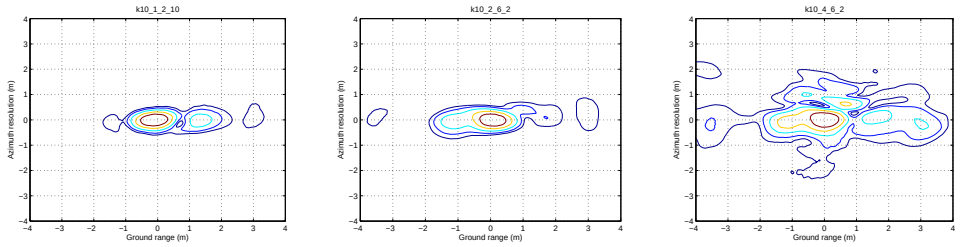

(a) (b) (c)

Figure 13. Examples of trihedral responses. Contour levels are -3dB (red), -6dB (yellow), -10dB (light blue), -15dB (dark blue) and -20dB (black). (a) is a monostatic example and (b) and (c) are bistatic examples. (a)-(b) is from deployment A and (c) is from deployment B, see Figure 5. The -3 dB width is approximately the same in all examples.

5.5 Detection of vehicles concealed in forest

The concealed vehicles were deployed in a moderately topographic forest terrain of about 600 m x 600 m, i.e. the area confined by the yellow square in Figure 5. The range of the ground height undulations is 22 m and the selected area contains both sloping and flat conditions.

The forest clutter suppression, obtained by using a bistatic separation in elevation angle, is expected to be most pronounced when the tree trunks are standing on a flat surface, i.e. when the angle between the ground and trunk is close to 90°. An example of this is shown in Figure 14 with two TGB30 terrain vehicles located in the middle part of the forested area. The two vehicles are more visible with increasing bistatic angle both in the colour coded image chips and in the corresponding change images generated by the change detection algorithm [7]. The colour coded images have been generated by modulating the red channel with the SAR images acquired during deployment A, and the green and blue channels with the same registrations but from deployment B. Consequently, targets from deployment A are expected to become red while targets from deployment B will become turquoise. Clutter signals present in both deployments are assigned to all three colours and will thus appear as gray. The dynamic range is automatically set by the minimum and maximum pixel values present in each overview scene and the brightness of the images is hereby equalized. Hence, the results show that the forest clutter levels are reduced in favour of detecting the two TGB30 vehicles.

Another example is given in Figure 15 where a TGB30 vehicle is equally visible independent of the bistatic elevation angle. The local terrain is sloping in this example and the clutter levels in fact become stronger with increasing angles. The result for this specific target signature could be explained by the fact that the target radar cross section is also enhanced due to the bistatic angle and the sloping terrain.

When comparing the monostatic and “quasi-monostatic” results in Figure 14 and Figure 15 we observe that the monostatic images appear more gray compared to the “quasi-monostatic” images. This indicates better image matching for the monostatic images and that the bistatic performance could be enhanced in the future.

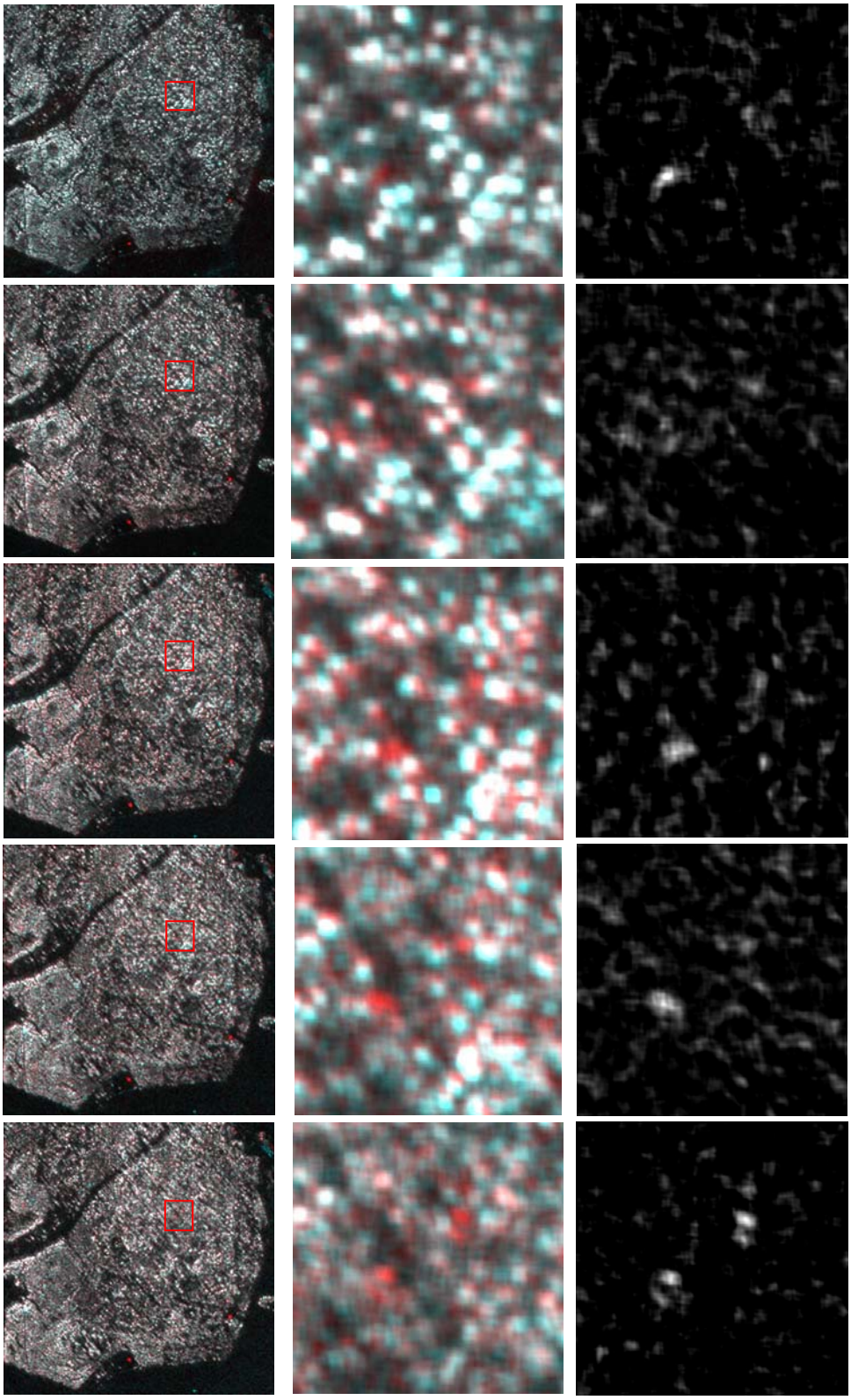

Figure 14. Example of two TGB30 imaged in the forested area. Red colour represents deployment A whereas the combination of green and blue (turquoise) corresponds to deployment B. The flight heading is 225°. From left to right; a) geo-referenced overview of the 600 m x 600 m forested area, b) zoom in of the area marked by the red square, c) resulting change image generated from the corresponding image pair. Images from top to bottom; I) true monostatic, II) “quasi-monostatic” (bistatic angle 0°), III) bistatic angle 3°, IV) bistatic angle 6° and V) bistatic angle 10°.

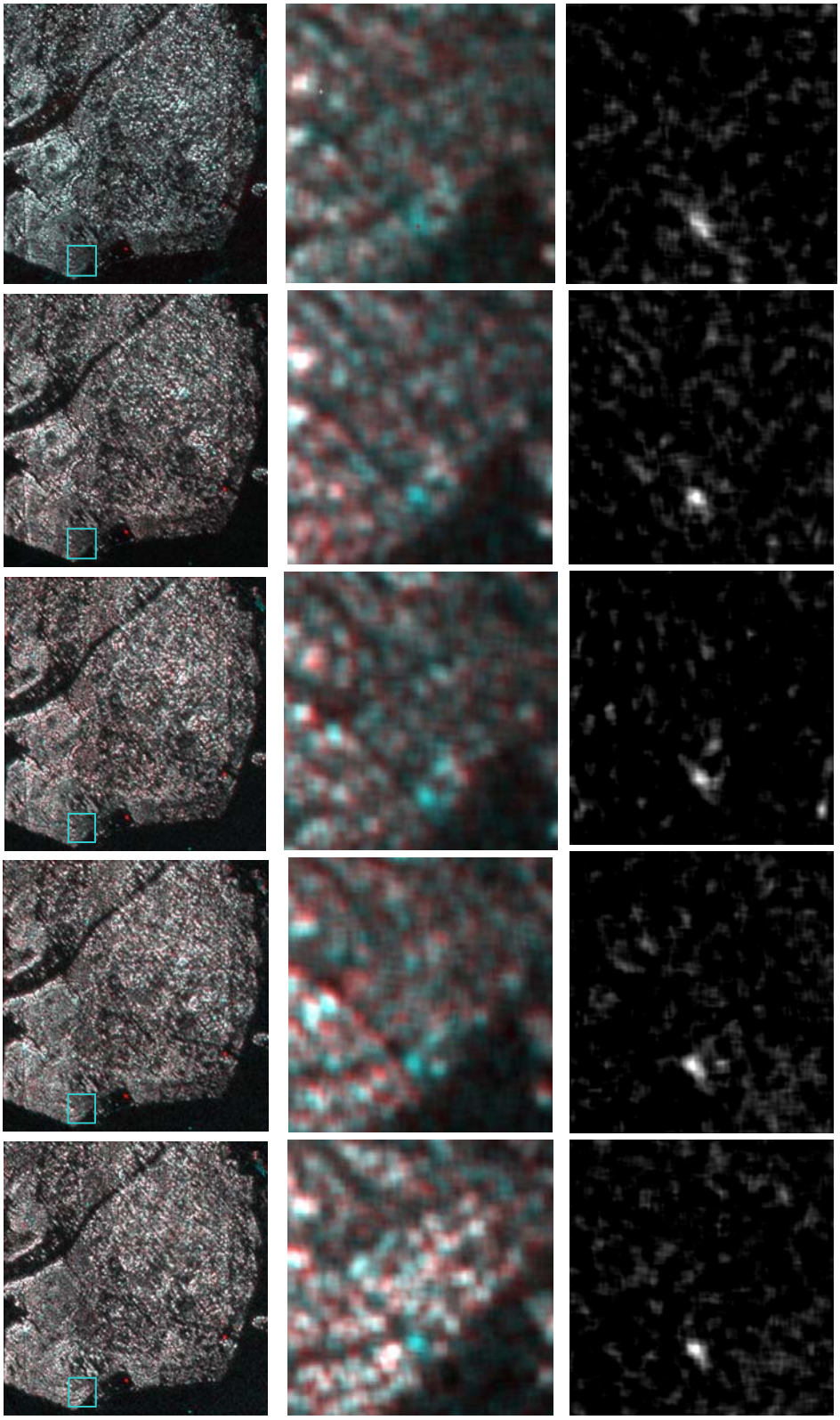

Figure 15. Example of one TGB30 imaged in the forested area. Red colour represents deployment A whereas the combination of green and blue (turquoise) corresponds to deployment B. Flight heading is 225°. From left to right; a) geo-referenced overview of the 600 m x 600 m forested area, b) zoom in of the area marked by the turqoise square, c) resulting change image generated from the corresponding image pair. Images from top to bottom; I) true monostatic, II) “quasi-monostatic” (bistatic angle 0°), III) bistatic angle 3°, IV) bistatic angle 6° and V) bistatic angle 10°.

Although a significant forest clutter reduction (mainly from ground-trunk scattering) is observed in the bistatic images, direct target detection performance based on a single image only remains poor. This is due to a high residual false alarms rate. Using change detection techniques, target detection performance is markedly improved in the monostatic case. However, less improvement was observed for the bistatic cases compared to the monostatic case and is probably related to the insufficient matching of the image pairs.

5.6 Imaging of buildings

In this section we include examples of imaging buildings in an urban area. The area is from the MOUT (military operation in urban terrain) under construction in Kvarn. The buildings are in different stages of being completed, i.e some have only been partly erected and lack a roof whereas others are close to completion. Figure 16a-b shows an example of one monostatic and one bistatic SAR image. Photos of the buildings are also shown in Figure 16c and Figure 17. The SAR images indicate that the radar wave is able to penetrate through the roof since a bright double-bounce signature is located both in the front and the back of that building. The latter indicates that penetration inside the building is significant since no other structure is visible in Figure 17 which could explain the strong double-bounce. Interior structures are also visible of this building, in particular in the bistatic SAR image where the metallic structure shown in Figure 16b is clearly delineated as a linear structure in the centre of the building. The surrounding smaller buildings do not show a corresponding signature and they do not contain any structures inside. Further work is needed to fully understand the building signatures.

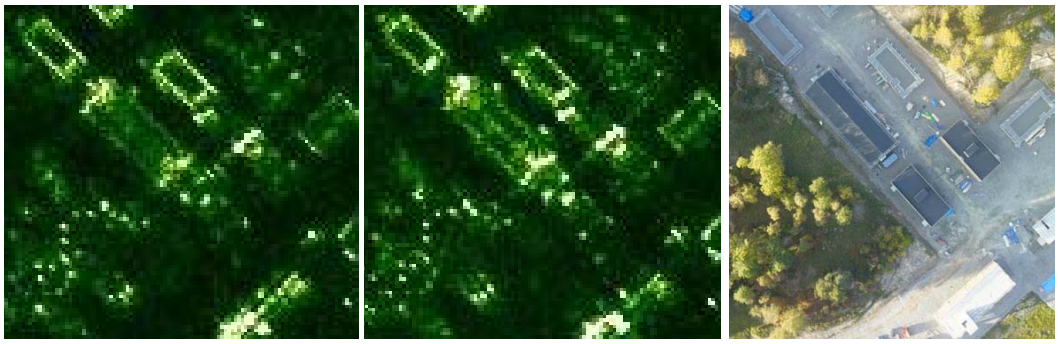

(a) Mission 1 Pass 2 (b) Mission 2 Pass 4 (c) Helicopter photo

Figure 16. Kvarn test site. The building in the centre of each image has a non-metallic roof. (a) Monostatic LORA image. (b) Bistatic image with elevation angle difference 3°. LORA is receiver and SETHI is transmitter. Flight heading is 225° and radar antenna is left looking for both images. (c) Helicopter photo. The image size is 0.1 km x 0.1 km. Note that the metallic interior structure of the building in Figure 17b is more clearly visible in the bistatic image.

(a) (b) (c)

Figure 17. (a)-(b) are ground photos of the building with non-metallic roof in the centre of the images in Figure 16. (c) is a photo of one of the surrounding buildings under construction.

6 Conclusions

The report summarises the highlights from the four-year research collaboration (2008-2011) on “Joint Bistatic Low Frequency Airborne Radar Experiments” between DGA and ONERA in France and FOI in Sweden.

An important outcome of the research project is that it is the first time that bistatic SAR images have been produced in the VHF/UHF-band (222-460 MHz) using two airborne platforms. This was accomplished during the preliminary flight tests in France 2009. Synchronization was established using a combination of system upgrades, including GPS-disciplined oscillators and phase drift corrections based on recording of the direct signal.

The main flight campaign was conducted in Sweden 2010 including an extensive target deployment. 17 vehicle targets ranging from personal car to truck-sized terrain vehicles were deployed at the Swedish Army Combat School Kvarn for the FOPEN experiment. Most vehicles were hidden under foliage but a few were positioned in open fields. Two deployments were used with target relocation in between in order to enable change detection analysis. Four flight missions were completed over Kvarn, i.e. two for each deployment.

Most of the bistatic imaging was conducted using parallel but offset tracks of the two aircraft. The two aircraft were in most cases flying side-by-side with the same speed and with one of the radars transmitting while both receiving the returned signal. Different bistatic elevation angles were obtained by offsetting the tracks from each other. In this manner, bistatic angles between 0° (“quasi-monostatic”) and 10° were realised. A few other geometries were also used including circular tracks, combinations of circular and straight tracks as well as parallel tracks with different speeds, but results have not yet been completed for these cases.

A second test site Remningstorp was also covered in one flight mission although no target deployment was prepared at this site. The reason for including Remningstorp was that there exits extensive ground truth to facilitate image interpretation of forest clutter.

The main result from processing and analysing the bistatic SAR images at horizontal polarization from Kvarn and Remningstorp is a significant decrease of the strong forest clutter levels due to reduced double-bounce scattering. The effect is more pronounced when the bistatic elevation angle increases and results show a suppression of up to 10 dB. The target radar cross section is less sensitive to the bistatic elevation angle due to its lower height which means that the target-to-clutter ratio is expected to increase. The latter is true in most cases but sometimes the opposite is observed which is caused by a sloping ground surface which locally may cause the double-bounce forest scattering to increase. Image examples from the two target deployments generally show increased visibility of the larger concealed vehicles in the bistatic SAR geometries but the smaller concealed vehicles were not possible to discriminate.

It has not been possible to complete the receiver-operating-characteristic (ROC) analysis as planned due to residual image geometrical distortions which limits change detection performance. The cause of this problem is not fully understood at present but is likely due to uncompensated phase drift between the two systems. The direct signal is used to measures the phase drift but is limited by fading of the signal through the antenna backlobe. For future bistatic experiments, it is recommended to develop means to minimise the direct signal fluctuations.

It was originally planned that some targets would be deployed inside a MOUT training site but this turned out not to be possible since construction activities were still going on. The MOUT area was nevertheless covered by the SAR images and provides an opportunity to study imaging of buildings. Results show that penetration through buildings and imaging of building interior structures is possible using VHF/UHF-band SAR, but requires that the roofing is non-metallic.

7 References

[1] Technical Arrangement 4.5, Joint Bistatic Low Frequency Airborne Radar Experiments, FOI Dnr 08-330, 2008.

[2] N.J. Willis, Bistatic Radar, Artech House, 1991.

[3] N.J. Willis and H.D. Griffiths (Eds.), Advances in Bistatic Radar, SciTech Publishing Inc., 2007.

[4] P. Dubois-Fernandez, H. Cantalloube, B. Vaizan, G. Krieger, R. Horn, M. Wendler, and V. Giroux, "ONERA-DLR bistatic SAR campaign: Planning, data acquisition, and first analysis of bistatic scattering behaviour of natural and urban targets," IEE Proc.-Radar Sonar Navig., vol. 153, no. 3, pp. 214-223, 2006.

[5] M. Rodriguez-Cassola, S.V. Baumgartner, G. Krieger, and A. Moreira, "Bistatic TerraSAR-X/F-SAR spaceborne–airborne SAR experiment: Description, data processing, and results," IEEE Trans. Geosci. Remote Sens. vol. 48, no. 2, pp. 781-794, 2010.

[6] L.M.H. Ulander, P.O. Frölind, A. Gustavsson, H. Hellsten, and B. Larsson, "Detection of concealed ground targets in CARABAS SAR images using change detection", Proc. Algorithms for Synthetic Aperture Radar Imagery VI, Orlando, FL, 5-9 April 1999, SPIE vol. 3721, pp. 243-252, 1999.

[7] L.M.H. Ulander, M. Lundberg, W. Pierson, and A. Gustavsson, "Change detection for low-frequency SAR ground surveillance," IEE Proc.-Radar Sonar Navig., vol. 152, no. 6, pp. 413-420, 2005.

[8] M.E. Davies, Foliage Penetration Radar, Detection and Characterization of Objects Under Trees, SciTech Publishing Inc., 2011.

[9] M. Lundberg, L.M.H. Ulander, W.E. Pierson, and A. Gustavsson, "A challenge problem for detection of targets in foliage," Proc. Algorithms for Synthetic Aperture Radar Imagery XIII, Orlando, FL, 17-21 April 2006, SPIE vol. 6237, pp. 62370K-1 - 62370K-12, 2006.

[10] W. Ye, C. Paulson, D.O. Wu, and J. Li, "A target detection scheme for VHF SAR ground surveillance," Proc. Algorithms for Synthetic Aperture Radar Imagery XV, Orlando, FL, 16-20 March 2008, SPIE vol. 6970, pp. 69700Y-1 - 69700Y-12, 2008.

[11] W. Ye, C. Paulson, D.O. Wu, and J. Li, "A rotation-invariant transform for target detection in SAR images," Proc. Algorithms for Synthetic Aperture Radar Imagery XV, Orlando, FL, 16-20 March 2008, SPIE vol. 6970, pp. 69700W-1 - 69700W-11, 2008.

[12] L. Novak, "FOPEN change detection experiments using a CARABAS public release data set," Proc. Algorithms for Synthetic Aperture Radar Imagery XVII, Orlando, FL, 5-9 April 2010, SPIE vol. 7699, pp. 76990V-1 - 76990V-10, 2010.

[13] L.M.H. Ulander, B. Flood, P.-O. Frölind, A. Gustavsson, T. Jonsson, B. Larsson, M. Lundberg, D. Murdin, and G. Stenström, "Change detection of vehicle-sized targets in forest concealment using VHF- and UHF-band SAR," IEEE AES Systems Magazine, vol. 26, no. 7, pp. 30-36, 2011.

[14] A. Jänis, S. Nilsson, L.-G. Huss, M. Gustafsson, and A. Sume, "Through-the-wall imaging measurements and experimental characterization of wall materials," Proc. Military Remote Sensing, London, UK, 27-28 October 2004, SPIE vol. 5613, pp. 67-75, 2004.

[15] E.J. Baranoski, "Through-wall imaging: Historical perspective and future directions," Journal of the Franklin Institute, vol. 345, no. 6, pp. 5173-5176, 2008.

[16] M. Gustafsson, “Reflection and transmission of reinforced concrete between 0-4 GHz: Calculations using FDTD,” FOI Technical report, FOI-R--2567--SE, Linköping, Sweden, 2008.

[17] M. Gustafsson and L.M.H. Ulander, “Monostatic and bistatic SAR-imaging study: Simulations using physical optics,” FOI Scientific report, FOI-R--2560--SE, Linköping, Sweden, 2008.

[18] L.M.H. Ulander and T. Martin, “Bistatic ultra-wideband SAR for imaging of ground targets under foliage, Proc. 2005 IEEE International Radar Conference, Arlington, VA, 9-12 May 2005, pp. 419-423, 2005.

[19] L.M.H. Ulander, A. Barmettler, B. Flood, P.-O. Frölind, A. Gustavsson, T. Jonsson, E. Meier, J. Rasmusson, and G. Stenström, “Signal-to-clutter ratio enhancement in bistatic very high frequency (VHF)-band SAR images of truck vehicles in forested and urban terrain,” IET Radar Sonar and Navigation, vol. 4, no. 3, pp. 438-448, 2010.

[20] R. Baqué, P. Dreuillet, O. Ruault du Plessis, H. Cantalloube, L. Ulander, G. Stenström, T. Jonsson, and A. Gustavsson, “LORAMbis. A bistatic VHF/UHF SAR experiment for FOPEN,” Proc. 2010 IEEE Radar Conference, Washington, D.C., 10-14 May 2010, pp. 832-837, 2010.

[21] G. Bonin and P. Dreuillet, “The airborne SAR-system: SETHI. Airborne microwave remote sensing imaging system,” Proc. EUSAR 2008, 7th European Conference on Synthetic Aperture Radar, Friedrichshafen, Germany, 2-5 June 2008, pp. 199-202, 2008.

[22] L.M.H. Ulander, M. Blom, B. Flood, P. Follo, P.-O. Frölind, A. Gustavsson, T. Jonsson, B. Larsson, D. Murdin, M. Pettersson, U. Rääf, and G. Stenström, “The VHF/UHF-band LORA SAR and GMTI System,” Proc. Algorithms for Synthetic Aperture Radar Imagery X, Orlando, FL, 21-23 April 2003, SPIE vol. 5095, pp. 206-215, 2003.

[23] T. Jonsson and G. Stenström, “Synchronization tests with LORA and SETHI SAR sensors,” FOI Memo 2830, Linköping, Sweden, 2009.

[24] A. Gustavsson, L.M.H. Ulander, P.O. Frölind, T. Jonsson, B. Larsson, G. Stenström., D. Le Coz, O. Du Plessis, and P. Martineau, “The French-Swedish Multi-Frequency SAR Campaign RAMCAR98”, Proc IGARSS’99, Hamburg, Germany, 28 June - 2 July 1999, pp. 2599-2603, 1999

[25] A. Gustavsson, L.M.H. Ulander, P.-O. Frölind, B. Hallberg, G. Smith-Jonforsen, P. Dreuillet, P. Dubois-Fernandez, and O. Ruault du Plessis, “LORAM – A SAR/GMTI data collection campaign,” Proc. EUSAR 2006, 6th European Conference on Synthetic Aperture Radar, Dresden, Germany, 16-18 May 2006, 4 pages, 2006.

[26] L.M.H. Ulander, H. Hellsten, and G. Stenström, “Synthetic-aperture radar processing using fast factorised back-projection,” IEEE Trans. Aerospace and Electronic Systems, vol. 39, no. 3, pp. 760-776, 2003.

[27] L.M.H. Ulander, P.-O. Frölind, A. Gustavsson, D. Murdin, and G. Stenström, “Fast factorized back-projection for bistatic SAR processing,” Proc. EUSAR 2010, 8th European Conference on Synthetic Aperture Radar, Aachen, Germany, 7-10 June 2010, pp. 1002-1005, 2010.

[28] L.M.H. Ulander, R. Baqué, H. Cantalloube P. Dreuillet, B. Flood, P.-O. Frölind, A. Gustavsson, T. Jonsson, B. Larsson, D. Murdin, R. Ragnarsson, O. Ruault du Plessis, and G. Stenström, “Observations of clutter suppression in bistatic VHF/UHF-band synthetic-aperture radar,” Proc. Algorithms for Synthetic Aperture

Radar Imagery XVIII, Orlando, FL, 25-29 April 2011, SPIE vol. 8051, pp. 80510H-1 - 80510H-9, 2011.

[29] H.M.J. Cantalloube, C. Coulombeix, and C.E. Nahum, “Processing of wide-band non-stationary bistatic airborne SAR signal from the Lorambis experiment,” Proc. IRS 2011, International Radar Symposium 2011, Leipzig, Germany, 7-9 September 2011, pp. 47-52, 2011.